analytical chemistry

Article

pubs.acs.org/ac

Ionophore-Based Voltammetric Ion Activity Sensing with Thin Layer Membranes

Maria Cuartero, Gaston A. Crespo,* and Eric Bakker*

Department of Inorganic and Analytical Chemistry, University of Geneva, Quai Ernest-Ansermet 30, CH-1211 Geneva, Switzerland

Supporting Information

ABSTRACT: As shown in recent work, thin layer ion-selective multi-ionophore membranes can be interrogated by cyclic voltammetry to detect the ion activity of multiple species simultaneously and selectively. Additional fundamental evidence is put forward on ion discrimination with thin multi-ionophore-based membranes with thicknesses of 200 ± 25 nm and backside contacted with poly-3-octylthiophene (POT). An anodic potential scan partially oxidizes the POT film (to POT^+), thereby initiating the release of hydrophilic cations from the membrane phase to the sample solution at a characteristic potential. Varying concentration of added cation-exhanger demonstrates that it limits the ion transfer charge and not the deposited POT film. Voltammograms with multiple peaks are observed with each associated with the transfer of one type of ion (lithium, potassium, and sodium). Experimental conditions (thickness and composition of the membrane and concentration of the sample) are chosen that allow one to describe the system by a thermodynamic rather than kinetic model. As a consequence, apparent stability constants for sodium, potassium, and lithium (assuming 1:1 stoichiometry) with their respective ionophores are calculated and agree well with the values obtained by the potentiometric sandwich membrane technique. As an analytical application, a membrane containing three ionophores was used to determine lithium, sodium, and potassium in artificial samples at the same location and within a single voltammetric scan. Lithium and potassium were also determined in undiluted human plasma in the therapeutic concentration range.

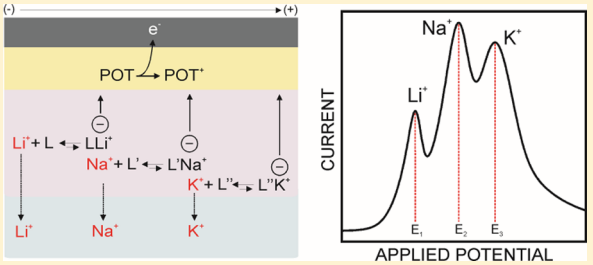

All solid-state ion-selective electrodes constructed with faradaic ion-to-electron transducing materials, such as poly(3-octylthiophene) (POT),[1−4] poly(3,4-ethylenedioxythiophene) (PEDOT),[5−10] polypyrrole,[11] 7,7,8,8-tetracyanoquinodimethane (TCQN),[12] tetrathialfulvane (TFN),[13] tetrathionaphtalene,[14] or ferrocene (Fc),[12,15,16] have offered the possibility of controlling electrochemical reactions (i.e., oxidation of POT to POT^+) at the inner interface of the electrode, thereby triggering an ion transfer reaction across the membrane/sample interface.

Early experiments performed by Si et al.[2] were mainly focused on using cyclic voltammetry for the establishment of a reversible ion-transfer process at very thin membranes (10 times thinner than previous systems).[1,3,5] A submicrometer thick membrane (~340 nm) containing plasticized PVC (PVC−DOS) and a mixture of cation and anion exchangers backside contacted with POT film was initially explored. Importantly, a reversible Gaussian peak shape was obtained as a voltammetric output signal. Both peaks were attributed to the depletion (anodic scan) and extraction (cathodic scan) of sodium into and from the membrane.

With the aim of developing ion-selective sensors, similarly formulated membranes (~200 nm) containing only lipophilic cation-exchanger and an ionophore selective either for lithium or calcium have recently been described by our group.[4] A significant shift of the voltammetric peak to most positive potentials was observed by adding the analyte (Ca^{2+} or Li^+) to the sample electrolyte. This was ascribed to a decrease of the thermodynamic free energy of the ionophore-analyte complex compared to that for the extraction of uncomplexed analyte. A more positive applied potential is therefore required to displace cationic analyte from the membrane. The difference in the peak potentials in the absence and presence of the primary analyte in the sample allowed one to calculate selectivity coefficients. Moreover, it was found that the peak potential position followed a linear relationship with the logarithm of the ion activity in the sample phase (from 10^{-5} to 0.1 M) in complete analogy to the potentiometric readout. In fact, this trend had also been observed earlier with other transducing materials, such as TFN[13] or TCQN,[12] although well-defined Gaussian peaks were not obtained in those cases. With POT, the integrated charge of each forward/backward Gaussian voltammetric peak was independent of analyte concentration in the above-mentioned range. The transported charge across the interface corresponded to a conversion of approximately 27% POT.[4]

These pieces of evidence indicate that (i) the oxidation of POT may be considered a surface-confined process, (ii) the depletion or extraction of the primary analyte into the

Received: September 23, 2015
Accepted: December 29, 2015
Published: December 29, 2015

DOI: 10.1021/acs.analchem.5b03611
Anal. Chem. 2016, 88, 1654−1660

membrane is a very rapid process (around 20 ms, using a film thickness of 200 nm and diffusion coefficient of 10^{-8} cm^2 s^{-1}),[17] and (iii) the membrane/sample interface is approximately at thermodynamic equilibrium for the mentioned concentration range. Considering these assumptions, a simplified theory based on equilibrium conditions was put forward[4] that avoided the necessity of including diffusion coefficients.

We note that at lower sample concentrations (typically lower than 10 μM), mass transport in the sample phase may become rate limiting. Under these conditions, the system may be treated as an analogy to that reported by Amemiya[1,3,5−7] in which very low limits of detection were realized for perchlorate, potassium, and protamine by thin film-based ionophore-based membranes. That methodology related to traditional stripping voltammetry at metal electrodes as the analyte is selectively accumulated in the polymeric film before the voltammetric stripping step.

According to the thermodynamic behavior found at relatively high concentrations,[4] the ionophore-based membrane can be described in some analogy to that under zero current conditions and allow one to observe Nernstian response slopes and to calculate selectivity coefficients. Indeed, Amemiya et al. recently used this thermodynamic approach to calculate stability constants for different binding stoichiometries in the membrane phase.[8] Accordingly, the applied potential may add a second readout dimension with respect to classical potentiometric measurements. For this reason, the incorporation of two ionophores in the very same membrane recently resulted in the first evidence of multianalyte selectivity.[4] Two well-resolved Gaussian peaks for lithium and calcium were observed, each following a Nernstian response behavior with analyte concentration in the sample.

We report here on two key findings that build on these exciting results. On the one hand, thin layer membranes are used for the calculation of thermodynamic parameters (i.e., formation constants of the analyte−ionophore complex in the membrane) can be compared to the established sandwich membrane technique.[18] On the other hand, they are demonstrated to be an attractive technology for multianalyte ion detection. To this end, we explore the limits of incorporating multiple ionophores (up to four) in the same membrane. The promise of the proposed approach to clinical analysis is evidenced by the direct detection of potassium and lithium activity in undiluted human serum.

EXPERIMENTAL SECTION

Reagents, Materials, and Equipment. Aqueous solutions were prepared by dissolving the appropriate chloride salts (Supporting Information) (Sigma-Aldrich) in deionized water (>18 MΩ cm). Lithium perchlorate ($LiClO_4$, >98%), 3-octyltiophene (97%), high molecular weight poly(vinyl chloride) (PVC), bis(2-ethylhexyl)sebacate (DOS), *o*-nitrophenyloctyl ether (NPOE), sodium tetrakis[3,5-bis(trifluoromethyl)phenyl]borate (NaTFPB), lithium ionophore VI, sodium ionophore X, potassium ionophore I, calcium ionophore IV, sodium chloride (NaCl), lithium chloride (LiCl), potassium chloride (KCl), calcium chloride ($CaCl_2$), tetrabutylammonium hexafluorophosphate (Bu_4NPF_6), tetrahydrofuran (>99.9%, THF), nitrobenzene (≥99.0%), and acetonitrile (anhydrous, >99.8%) were purchased from Sigma-Aldrich.

Synthetic samples for lithium analysis were prepared by mimicking the levels of magnesium, potassium, calcium, and sodium present in human plasma (20, 130, 110, and 3300 μg mL^{-1}, respectively).[19] Human plasma samples were provided by Hôpitaux Universitaires de Genève (HUG).

Au-electrode tip (6.1204.320) and GC-electrode tip (6.1204.300) with an electrode diameter of 3.00 ± 0.05 mm were sourced from Metrohm (Switzerland). Cyclic voltammograms were recorded with a PGSTAT 302N (Metrohm Autolab B.V., Utrecht, The Netherlands) controlled by Nova 1.10 software (supplied by Autolab) running on a PC. A double-junction Ag/AgCl/3 M KCl/1 M LiOAc reference electrode (6.0726.100 model, Metrohm, Switzerland) and a platinum electrode (6.0331.010 model, Metrohm, Switzerland) were used in the three-electrode cell. A rotating disk electrode (Autolab RDE, Metrohm Autolab B.V., Utrecht, The Netherlands) was used to spin coat the membranes on the electrodes at 1500 rpm.

Preparation of the Electrodes. Poly(3-octylthiophene) (POT) was electrochemically polymerized on GC and Au surfaces by cyclic voltammetry (0−1.5 V, 100 mV s^{-1}, two scans for GC electrode and three scans for Au electrode) and then discharged at 0 V for 120 s. A solution containing 0.1 M 3-octylthiophene (OT) and 0.1 M $LiClO_4$ in acetonitrile was used. The solution was purged with N_2 for 30 min before use.[2] Following this, the electrode was immersed in pure acetonitrile for 30 min to remove the electrolyte and dried at room temperature for 15 min. Thereafter, a volume of 25 μL of diluted membrane cocktail (50 μL of the membrane cocktail + 150 μL of THF) was spin coated on the electrode. Table 1 shows the compositions of the membrane cocktails prepared in 1 mL of THF. Conditioning of the membranes was not deemed necessary (estimated equilibration time of ∼20 ms using a film thickness of 200 nm and diffusion coefficient of 10^{-8} cm^2 s^{-1}).[17]

Table 1. Ionophore-Based Membrane Compositions

		components					
membrane	PVC[a]	DOS[a]	NaTFPB[b]	Li-I[b]	Na-I[b]	K-I[b]	Ca-I[b]
I	30	60	40		80		
II	30	60	40			80	
III	30	60	40	80			
IV	30	60	40				
V	30	60	40	40		40	
VI	30	60	60	40	40	40	
VII	30	60	80	40	40	40	
VIII	30	60	100	40	40	40	
IX	30	60	68	40		40	
X	30	60	135	40	40	40	40

[a]Mass percentage. [b]mmol kg^{-1}; Li-I, Na-I, K-I, and Ca-I are lithium, sodium, potassium, and calcium ionophores, respectively.

RESULTS AND DISCUSSION

The use of membranes with thicknesses of hundreds of nanometers[2,4] backside contacted with POT and coupled to a potential-time dependence technique, such as voltammetry, has recently resulted in a novel sensing platform with two unprecedented key points: (i) use of a second discrimination dimension given by the linear sweep potential and (ii) understanding the electrochemical process as an equilibrium surface confined reaction that is independent of mass transport kinetics.

DOI: 10.1021/acs.analchem.5b03611
Anal. Chem. 2016, 88, 1654−1660

As established recently,[4] the electrochemistry of the POT underlayer is responsible for controlling both the extraction and the release of the analyte ion into and from the thin layer ion-selective membrane. When POT is oxidized to POT^+ during the forward scan, it forms ion pairs with the cation exchanger ($TFPB^-$) present in the membrane phase, resulting in the expulsion of the corresponding cation (i.e., Na^+) and vice versa during the backward scan.

For rationalization of the role of both the conducting polymer and the cation exchanger in this system, the POT oxidation wave was studied separately from the ion-transfer at the sample−membrane interface as follows. The voltammetric characterization was performed at a glassy carbon electrode containing only a coating of POT (55 ± 1 nm of thickness measured by ellipsometry) and using a lipophilic salt (0.1 M Bu_4NPF_6) dissolved in nitrobenzene (ε = 34.8) to approximate the solvent conditions of an overlaying membrane (*o*-NPOE, ε = 23.9). Figure 1 shows the cyclic voltammograms obtained at

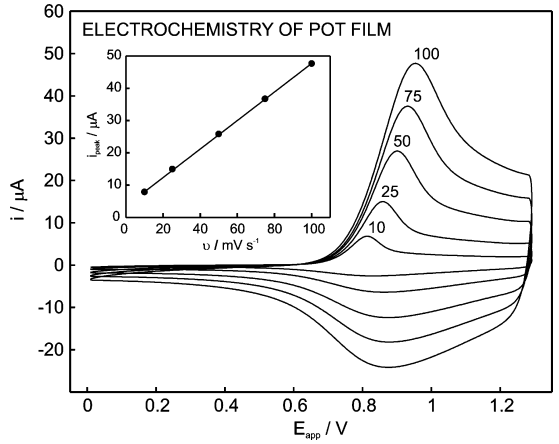

Figure 1. Observed cyclic voltammograms for 0.1 M Bu_4NPF_6 in nitrobenzene with a POT-based electrode conditioned for 24 h in the same solution at the indicated scan rates. Inset: peak current vs scan rate.

different scan rates in which the oxidation of POT is clearly visualized in the range of 700−950 mV. A significant capacitive current was observed after the anodic peak (about half the value of the peak current), suggesting a dramatic enlargement of the effective surface area of the conducting polymer upon oxidation. Both the Gaussian peak shape and the observed linearity with scan rate (inset of Figure 1) confirmed the confinement of the electrochemical process of POT by the incorporation of the lipophilic anion (NPF_6^-) in its lattice. Under such conditions, the concentration of the POT provides the maximum available charge in the system (i.e., 18.2 μC for 100 mV s^{-1}).

Subsequently, different ion-selective membranes with variable concentration of cation exchanger (from 20 to 300 mmol kg^{-1} in the undiluted cocktail) were spin coated on the conducting polymer layer. As expected, the concentration of cation exchanger in the membrane limited the oxidation of POT and consequently the resulting ion transfer charge (Figure 2a). We found that at 200 mmol kg^{-1} of cation exchanger the forward and backward ion-transfer peaks (13.9 μC out of the deposited 18.2 μC, ~76%) lose their Gaussian shape and widen significantly, which negatively impact the quality of the analytical signal. For this reason, experimental conditions

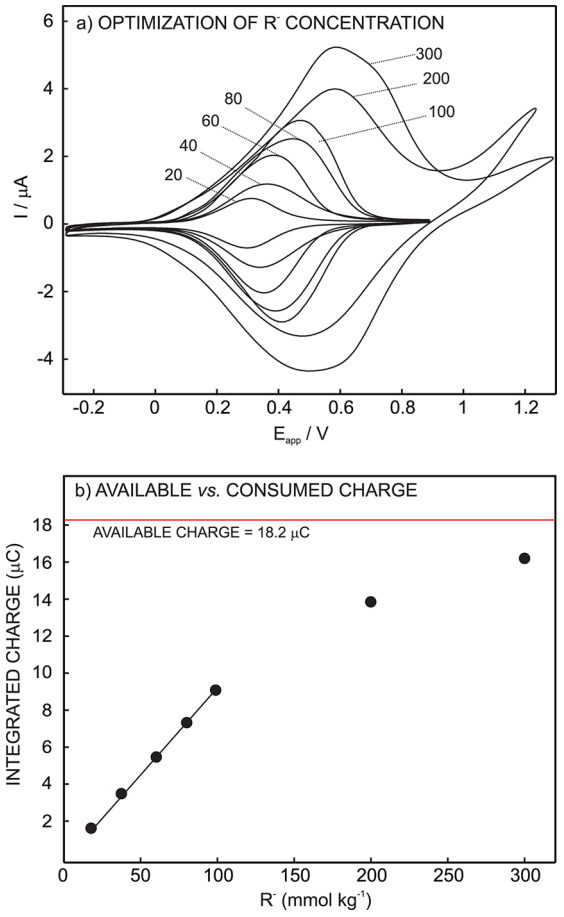

Figure 2. (a) Cyclic voltammograms obtained with membranes containing increasing amounts of the cation exchanger NaTFPB (from 20 to 300 mmol kg^{-1}). (b) Observed integrated charges for the ion-transfer process at different concentrations of NaTFPB. Red line indicates which is the maximum available charge in the system, given by the deposited charge of POT.

were selected in which only a small fraction of the available charge provided by the oxidation of POT is used. In the typical case of 40 mmol kg^{-1} cation exchanger, only 20% of POT is electrochemically converted (see Figure 2b).

Preliminary experiments with individual membranes containing sodium (labeled as MI, see Table 1), potassium (MII), and lithium (MIII) ionophores were characterized (Figure 3). For this purpose, cyclic voltammograms were recorded with different interfering and primary analyte ions to identify possible limitations in hypothetical physiological samples (see below). As expected, a Hofmeister selectivity pattern was observed for the control membrane (Figure SI-1) (lipophilicity order: Mg^{2+} < Ca^{2+} < Li^+ < Na^+ < K^+), whereas the incorporation of an ionophore produced a remarkable shift to higher potentials. Table 2 summarizes the potential shifts and the calculated resulting selectivity coefficients on the basis of the separate solution method (SSM).[20] The obtained values correspond to the reported ones with some discrepancies for the more discriminated cations, such as calcium and magnesium.[21]

The information obtained from Figure 3 was used to calculate apparent stability constants (primary analyte and ionophore, β) in the membrane phase analogously to the established sandwich membrane technique.[18,21] Assuming a 1:1 stoichiometry, the stability constants were calculated from the

DOI: 10.1021/acs.analchem.5b03611
Anal. Chem. 2016, 88, 1654−1660

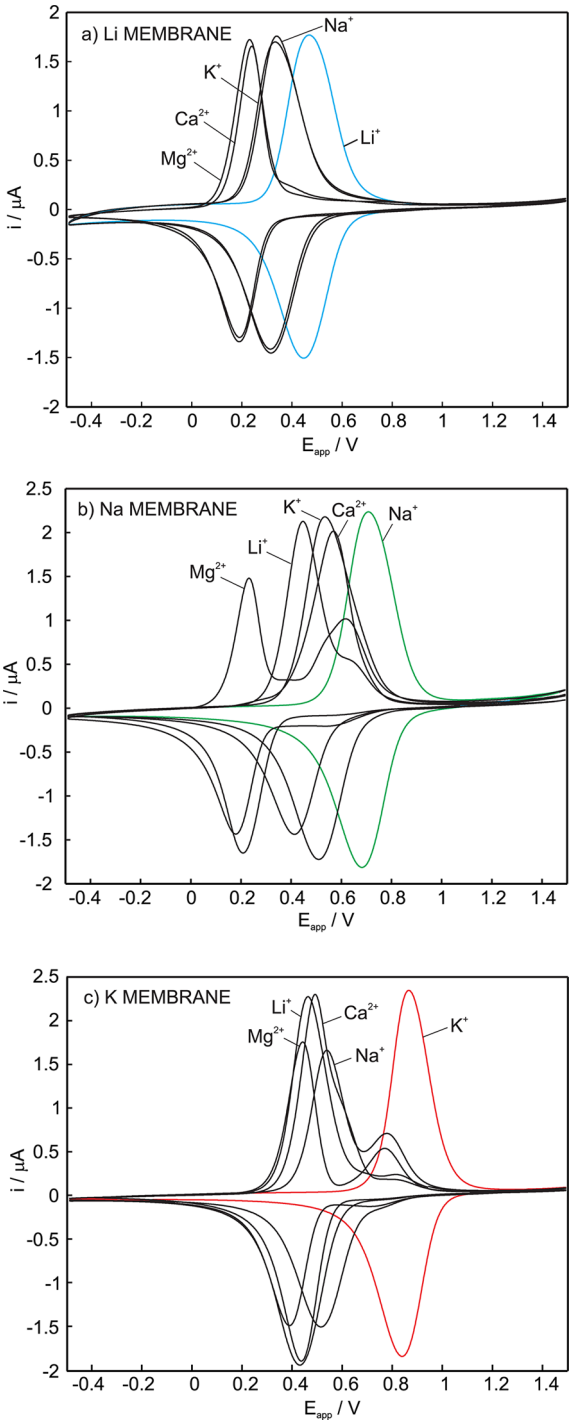

Figure 3. Cyclic voltammograms in separate 10 mM KCl, NaCl, LiCl, $CaCl_2$, and $MgCl_2$ solutions with the (a) lithium-selective membrane (MIII), (b) sodium-selective membrane (MI), or (c) potassium-selective membrane (MII). Scan rate: 100 mV s^{-1}.

peak potentials for the ion-transfer waves comparing membranes with and without ionophore. The observed potential shifts were 216.2 ± 5, 450.3 ± 4, and 561.4 ± 2 mV for lithium, sodium, and potassium selective membranes, respectively. The resulting logarithmic formation constants ($\log\beta_{LiL}$ = 4.66 ± 0.05;$\log\beta_{NaL'}$ = 8.62 ± 0.07, and $\log\beta_{KL''}$ = 10.49 ± 0.05) were in reasonable agreement with the reported values using potentiometry (4.37 ± 0.01, 7.69 ± 0.05, and 10.10 ± 0.07, respectively).[21]

Table 2. Calculated Selectivity Coefficients[a]

	log K_{IJ}				
membrane	J = Na^+	J = K^+	J = Li^+	J = Mg^{2+}	J = Ca^{2+}
sodium ionophore (I = Na^+)	0	−3.0	−4.5	−9.1	−3.3
potassium ionophore (I = K^+)	−5.6	0	−6.8	−8.1	−7.2
lithium ionophore (I = Li^+)	−2.2	−2.4	0	−5.0	−4.9
control (I = Na^+)	0	0.8	−0.2	−2.0	−2.2

[a]Standard deviations (n = 3) were lower than 0.1 in all cases.

Besides the usefulness of using this voltammetric approach to extract thermodynamic data, two remarkable points are noted. The first is related to the excellent reproducibility and reversibility of the extraction and release waves. Reproducibility is demonstrated by the insignificant variation of the peak current (~50 nA average) after 50 consecutive scans (see Figure SI-2), whereas a 0.5% variation between the calculated charges for forward and backward scans indicated the reversibility of the ion transfer process (e.g., 3.74 and 3.72 µC for sodium using MI). The similar charge values for individual peaks from a given membrane confirm that a constant amount of charge is always transferred (e.g., for MIII, calculated charges are 3.65 µC for Li^+, 3.64 µC for K^+, 3.64 µC for Na^+, 3.60 µC for Ca^{2+}, and 3.59 µC for Mg^{2+}).

Analogous to experiments with lithium-selective membranes,[4] the observed peak potentials for sodium and potassium (using MI and MII) shift to more positive values with increasing ion activity in agreement with the Nernst equation (Figure SI-3). The second point relates to the possibility of fabricating a membrane containing all three ionophores in view of multianalyte detection. This may be predicted from the peak potentials for the individual membranes, which were 488, 740, and 970 mV for 10 mM lithium, sodium, and potassium, respectively (see Figure 3).

Figure 4 shows the cyclic voltammograms for the optimal three ionophore-based membrane (MVIII) overlaid with those for each individual membrane (MI, MII, and MIII). The peak positions remain very similar in the multi-ionophore-based membrane (499, 762, and 1015 mV for lithium, sodium, and potassium) compared to the membranes containing just one

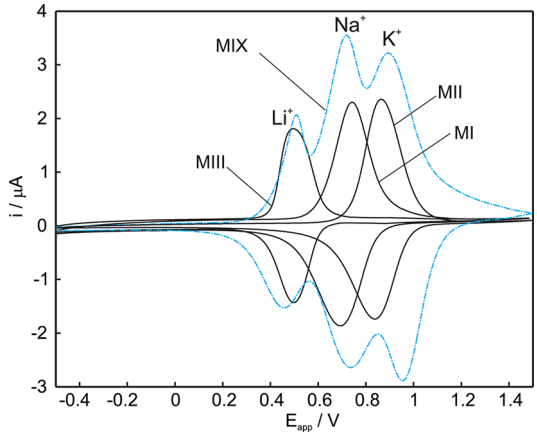

Figure 4. Cyclic voltammograms in a solution of 10 mM LiCl, NaCl, and KCl with membranes containing either single ionophores (MI, MII, and MIII) or three ionophores (MVIII). Background electrolyte: 10 mM $MgCl_2$. Scan rate: 100 mV s^{-1}.

DOI: 10.1021/acs.analchem.5b03611
Anal. Chem. 2016, 88, 1654−1660

ionophore. In principle, this indicates that a prior identification of the ion-transfer peak potential (by using a single ionophore membrane) is a useful estimator for designing a multi-ionophore membrane without overlapping peaks.

As an example, the incorporation of calcium ionophore (1040 mV) to MVIII may result in an overlap with the potassium peak (970 mV). This prediction was experimentally confirmed with a four ionophore-membrane (see Figure SI-4). Indeed, this membrane (MX) was not able to discriminate between potassium and calcium because of spontaneous, competitive ion-exchange between these two ions.

An optimization of the cation exchanger concentration for multi-ionophore-based membranes was required. Ideally, the membrane should contain the same molar concentration of cation exchanger (NaTFPB) as that of the combined ionophores in terms of their anticipated binding capacity. Figure 5 shows the observed cyclic voltammograms for an

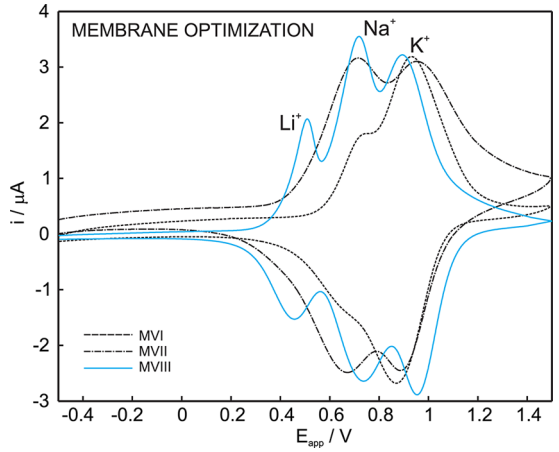

Figure 5. Cyclic voltammograms in a solution containing 10 mM LiCl, NaCl, and KCl (10 mM $MgCl_2$ background electrolyte) using membranes containing three ionophores with different compositions of MVI–MVIII. Scan rate: 100 mV s^{-1}.

increasing amount of cation exchanger (NaTFPB) while maintaining the same molar concentration of the three ionophores. A membrane containing half the amount of cation exchanger with respect to the sum of the three ionophores (MVI) only exhibited two ion transfer waves that correspond to sodium and potassium. Indeed, these two ions are preferably extracted compared to lithium and the low cation-exchanger concentration precludes the presence of lithium in the membrane at equilibrium. An increase of the cation exchanger concentration resulted first in an increase of the sodium peak (MVII) and only subsequently of the lithium peak (MVII). This last membrane (100:40:40:40 NaTFPB:LI-I:Na-I:K-I) was found to be optimal, and a further increase of the cation exchanger concentration neither improved nor deteriorated the membrane ion transfer characteristics. A thin layer behavior of the membrane was confirmed, as evidenced by the linear dependence of peak potential with scan rate (Figure SI-5).

Similar results were obtained with a membrane containing lithium and potassium ionophores (Figure SI-6). Here, the membrane containing a NaTFPB concentration of ~85% compared to the sum of the molar concentration of the ionophores (MIX) was found to be optimal. This may be adopted as a general protocol to fabricate multi-ionophore membranes for multianalyte detection. The experimentally observed deviation from the idealized case may be attributed to uncertainties during the weighing of the membrane components as well as the presence of impurities, including that of PVC that may act as additional cation exchanger sites.[22,23]

Figure 6a shows the observed cyclic voltammograms using membrane MVIII at different equimolar concentrations of

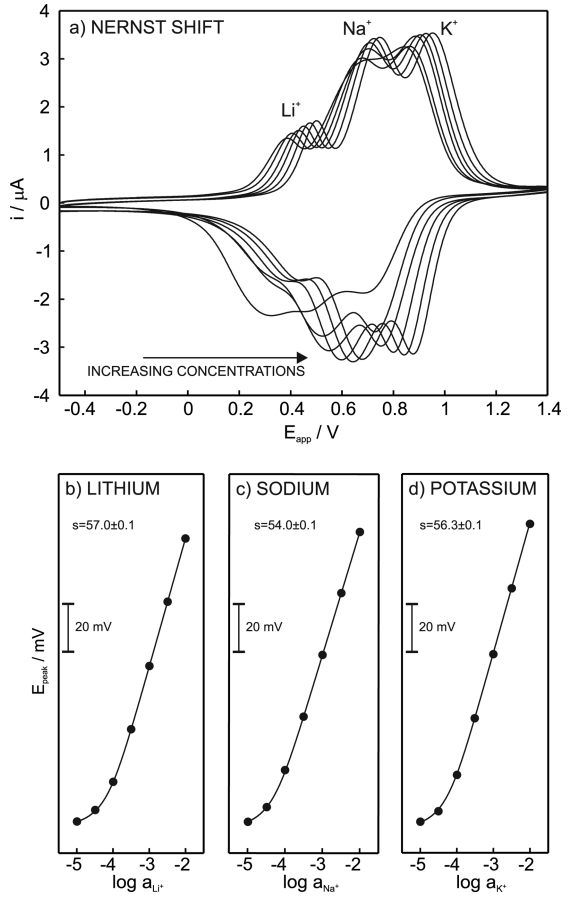

Figure 6. (a) Cyclic voltammograms for different concentrations of lithium, sodium, and potassium at equimolar concentrations (3.16×10^{-5}, 1×10^{-4}, 3.16×10^{-4}, 1×10^{-3}, 3.16×10^{-3}, 1×10^{-2} M) in 10 mM $MgCl_2$ background electrolyte with membrane MVIII on a gold electrode. (c) Observed calibration curves for lithium, sodium, and potassium. Scan rate: 100 mV s^{-1}.

lithium, sodium, and potassium. A gradual increase of each cation concentration resulted in a shift of peak potential to more positive values that agrees with a Nernstian behavior (Figure 6b–d). At low ion concentrations (Figure SI-7), the three peaks could not be distinguished, and it was not until a concentration of 3.16×10^{-5} M (close to LOD) that all three peaks started to be resolved and subsequently move to more positive values in agreement with the Nernst equation. The use of a different plasticizer for the membrane (*o*-NPOE) or another electrode material (Au) did not substantially alter the analytical performances of the sensors (Figure SI-8 and Table S1).

The proposed multianalyte sensors containing three ionophores were evaluated in artificial serum plasma and undiluted human plasma (see Experimental Section). Although three peaks were expected (for lithium, sodium, and potassium), only two peaks were visible (Figure SI-9a and b) owing to the overlap of the sodium and potassium transfer

DOI: 10.1021/acs.analchem.5b03611
Anal. Chem. 2016, 88, 1654–1660

waves. The 50-fold molar excess of sodium compared to potassium shifted the sodium transfer wave excessively in the direction of the potassium transfer wave (Figure SI-9c). Still, the membrane allowed one to obtain a calibration curve for lithium that followed the Nernst equation.

Similar results were observed with the optimized membrane MIX containing only lithium and potassium ionophores (Figure 7a). In this case, a calibration curve for potassium could be obtained at the same time as that for lithium (Figure SI-10) for a simultaneous determination of lithium and potassium in the sample (Figure 7b). The obtained linear range for lithium (Figure 7c) is suitable for its determination in samples of patients either under clinical treatment (0.4−1.0 mmol L^{-1})[24,25] or with harmful conditions (1.5−2.5 mmol L^{-1}).[26] This suggests that the principle put forward here may serve as a simple and reliable sensing strategy for the measurement of lithium blood levels under physiological conditions.

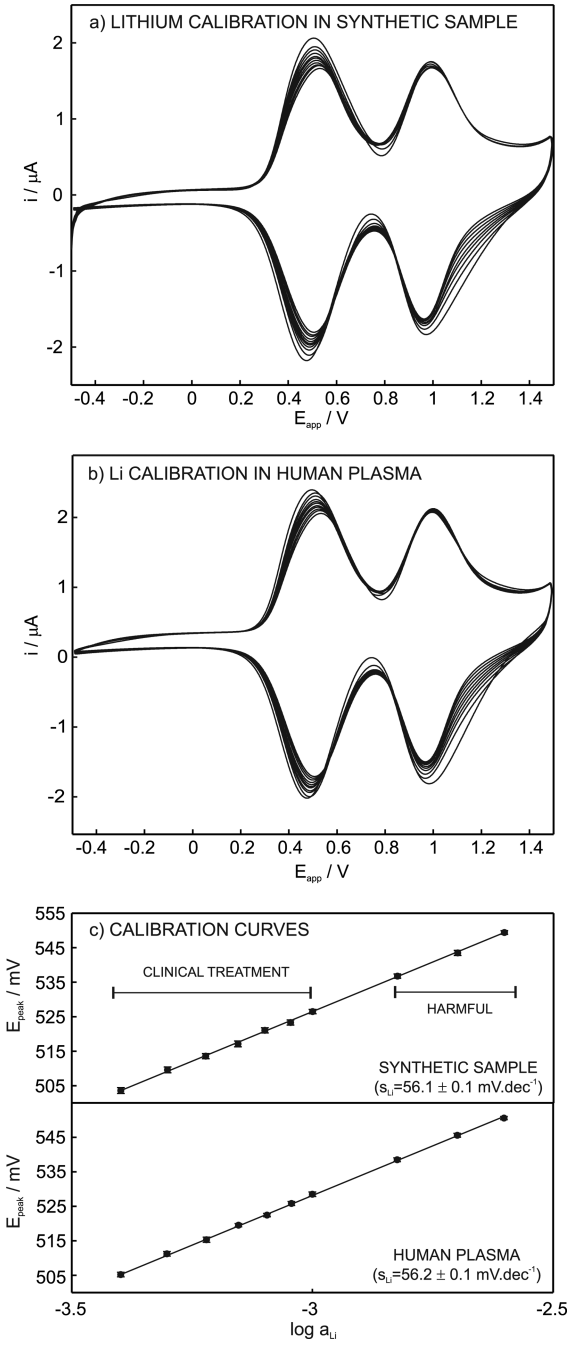

Figure 7. (a) Cyclic voltammograms in synthetic sample at increasing lithium activities using MVII containing lithium and potassium ionophores. (b) Cyclic voltammograms in human plasma at increasing lithium activities using MIX. (c) Calibration curves for lithium (first peak, n = 3). Scan rate: 100 mV s^{-1}.

CONCLUSIONS

A voltammetric multi-ionophore thin membrane concept for simultaneous multi-ion detection was further studied. As the system is interrogated under thermodynamic conditions (scan rate, thickness, and composition of the membrane and ion activity in the sample), ionophore-analyte complex formation constants and unbiased selectivity coefficients could be experimentally obtained. A careful optimization of membrane composition in terms of cation exchanger and ionophore molar ratio was performed. As a consequence, the simultaneous determination of several ions (up to three, lithium, sodium, and potassium) was achieved for the first time in synthetic samples using multi-ionophore-based membranes. The optimized membranes were subsequently characterized as a possible diagnostic tool for lithium in undiluted human plasma. In addition, the use of an optimized membrane based on two ionophores permits the simultaneous determination of lithium and potassium in synthetic and real plasma. Thin membrane layer ion transfer voltammetry may offer significant appeal for gaining fundamental insights into the ionophore-based membrane electrodes and for designing sensor devices capable of measuring ion activities of multiple ions at the very same location within a single, relatively rapid voltammetric scan. Further studies on the redox properties of POT in contact with an organic solvent that mimics the overcoated membrane will be useful to develop a more complete theoretical understanding of the behavior of the conducting polymer.

ASSOCIATED CONTENT

Supporting Information

The Supporting Information is available free of charge on the ACS Publications website at DOI: 10.1021/acs.analchem.5b03611.

Calibration parameters for different electrodes; selectivity for the control membrane; reproducibility; calibrations for sodium and potassium ion-selective membranes; response of a membrane containing four ionophores; evidence of thin layer behavior; sodium interference; electrode comparison; results with a membrane containing two ionophores; calibration graphs in artificial and human plasma (PDF)

AUTHOR INFORMATION

Corresponding Authors

*E-mail: gaston.crespo@unige.ch.
*E-mail: eric.bakker@unige.ch.

Notes

The authors declare no competing financial interest.

ACKNOWLEDGMENTS

The authors thank the Swiss National Science Foundation and the European Union (FP7-GA 614002-SCHeMA project) for supporting this research.

DOI: 10.1021/acs.analchem.5b03611
Anal. Chem. 2016, 88, 1654−1660

REFERENCES

(1) Guo, J.; Amemiya, S. *Anal. Chem.* **2006**, *78*, 6893−6902.
(2) Si, P.; Bakker, E. *Chem. Commun.* **2009**, 5260−5262.
(3) Kim, Y.; Amemiya, S. *Anal. Chem.* **2008**, *80*, 6056−6065.
(4) Crespo, G. A.; Cuartero, M.; Bakker, E. *Anal. Chem.* **2015**, *87*, 7729−37.
(5) Kim, Y.; Rodgers, P. J.; Ishimatsu, R.; Amemiya, S. *Anal. Chem.* **2009**, *81*, 7262−7270.
(6) Kabagambe, B.; Garada, M. B.; Ishimatsu, R.; Amemiya, S. *Anal. Chem.* **2014**, *86*, 7939−7946.
(7) Garada, M. B.; Kabagambe, B.; Amemiya, S. *Anal. Chem.* **2015**, *87*, 5348−5355.
(8) Greenawalt, P. J.; Garada, M. B.; Amemiya, S. *Anal. Chem.* **2015**, *87*, 8564−8572.
(9) Niu, L.; Kvarnstrom, C.; Dong, S.; Ivaska, A. *Synth. Met.* **2001**, *121*, 1389−1390.
(10) Han, D.; Yang, G.; Song, J.; Niu, L.; Ivaska, A. *J. Electroanal. Chem.* **2007**, *602*, 24−28.
(11) Shao, Y.; Jin, Y. D.; Wang, J. L.; Wang, L.; Zhao, F.; Dong, S. J. *Biosens. Bioelectron.* **2005**, *20*, 1373−1379.
(12) Zhang, J.; Harris, A. R.; Cattrall, R. W.; Bond, A. M. *Anal. Chem.* **2010**, *82*, 1624−1633.
(13) Harris, A. R.; Zhang, J.; Cattrall, R. W.; Bond, A. M. *Anal. Methods* **2013**, *5*, 3840−3852.
(14) Oyama, N.; Yamaguchi, S.; Shimomura, T. *Anal. Chem.* **2011**, *83*, 8429−8438.
(15) Jarolimova, Z.; Crespo, G. A.; Afshar, M. G.; Pawlak, M.; Bakker, E. *J. Electroanal. Chem.* **2013**, *709*, 118−125.
(16) Jarolimova, Z.; Crespo, G. A.; Xie, X. J.; Afshar, M. G.; Pawlak, M.; Bakker, E. *Anal. Chem.* **2014**, *86*, 6307−6314.
(17) Long, R.; Bakker, E. *Anal. Chim. Acta* **2004**, *511*, 91−95.
(18) Mi, Y. M.; Bakker, E. *Anal. Chem.* **1999**, *71*, 5279−5287.
(19) Nemutlu, E.; Ozaltin, N. *Anal. Bioanal. Chem.* **2005**, *383*, 833−838.
(20) Umezawa, Y.; Umezawa, K.; Sato, H. *Pure Appl. Chem.* **1995**, *67*, 507−518.
(21) Qin, Y.; Mi, Y. M.; Bakker, E. *Anal. Chim. Acta* **2000**, *421*, 207−220.
(22) Qin, Y.; Bakker, E. *Anal. Chem.* **2001**, *73*, 4262−4267.
(23) Horvai, G.; Graf, E.; Toth, K.; Pungor, E.; Buck, R. P. *Anal. Chem.* **1986**, *58*, 2735−2740.
(24) Albero, M. I.; Ortuno, J. A.; Garcia, M. S.; Cuartero, M.; Alcaraz, M. C. *Sens. Actuators, B* **2010**, *145*, 133−138.
(25) Novell, M.; Guinovart, T.; Blondeau, P.; Rius, F. X.; Andrade, F. J. *Lab Chip* **2014**, *14*, 1308−1314.
(26) Dale, M. M., Ritter, J. M., Gardner, P., Rang, H. P. *Pharmacology*, 4th ed.; Churchill Livingstone: UK, 2001.

DOI: 10.1021/acs.analchem.5b03611
Anal. Chem. 2016, 88, 1654−1660